JOURNAL OF MATERIALS SCIENCE 20 (1985) 3003–3010

Electron irradiation effects on interlaminar shear strength of glass or carbon cloth reinforced epoxy composites

N. TAKEDA*, S. KAWANISHI, A. UDAGAWA, M. HAGIWARA
Japan Atomic Energy Research Institute, Takasaki Radiation Chemistry Research Establishment, Takasaki-shi, Gunma 370-12, Japan

Interlaminar tensile shear tests are conducted to study the degradation mechanisms of electron irradiated glass or carbon cloth reinforced epoxy laminates. Interlaminar shear strength decreases significantly after the dose exceeds 3000 Mrad for glass/epoxy, but remains constant up to 12 000 Mrad for carbon/epoxy. SEM photos reveal that debonding of glass fibres and epoxy matrix (or degradation of silane coupling agents) plays an important role in the dose-dependent strength reduction of glass/epoxy laminates. The decrease in the interlaminar shear strength corresponds to that in the three-point bending strength. On the other hand, the SEM fracture appearance is almost dose-independent for carbon/epoxy laminates. In addition, some preliminary irradiation tests are conducted at −120° C to observe the effects of irradiation temperatures.

1. Introduction

Studies of radiation effects on the properties of fibre-reinforced plastics (FRP) composite materials have been attracting much interest recently. FRP materials are being increasingly used for large-scale structures in space, such as communication antennas and solar reflectors [1] and subjected to large doses of high-energy electrons and protons [1, 2]. Moreover, they are anticipated to be used for conductor insulation, thermal insulation, helium containers and other structures in the superconducting magnets for fusion reactors where they will be subjected to high fluxes of energetic neutrons and secondary gammas [3]. The main concerns are radiation-induced changes in mechanical and physical properties of FRP materials which affect the long-term durability. Several works have been reported on mechanical and electrical properties of FRP materials irradiated at low temperature [4–10]. However, the mechanism of radiation-induced degradation is not clear even for room temperature irradiation as well as for low temperature irradiation [11]. Understanding of the degradation mechanism is necessary to improve the radiation resistance of FRP materials.

According to the authors' previous three-point bending tests [11], it is known that degradation (or debonding) of matrix–fibre interfaces as well as matrix degradation is an important factor for the radiation resistance. For FRP laminates, in particular, the interfacial and matrix degradation result in the reduction of the interlaminar shear strength. In this paper, interlaminar tensile shear tests are conducted for glass or carbon cloth reinforced epoxy laminates irradiated by large-dose high-energy electrons. Degradation mechanisms are clarified by the combination of the scanning electron micrographs and the interlaminar shear strength data. The interlaminar shear strength is then compared and related with the three-point bending strength. Effects of electron irradiation temperatures are also briefly discussed.

Present address: Research Institute for Applied Mechanics, Kyushu University, Kasuga-shi, Fukuoka 816, Japan.

0022–2461/85 $03.00 + .12

2. Experiments – interlaminar tensile shear tests for electron irradiated FRP laminates

2.1. Tested materials

Glass or carbon fibre cloth reinforced epoxy composite laminates were prepared and denoted by G/E or C/E in the following paragraphs. The glass cloth is Kanebo Textoglass KS1210, E-glass plain-woven type, and consists of 53 yarns/25 mm in the warp direction and 48 yarns/25 mm in the fill direction. Each yarn consists of about 200 continuing fibres of 7 μm diameter. The carbon cloth is Torayc no. 6142 plain-woven type, and consists of 22.5 yarns/25 mm in both warp and fill directions. Each yarn consists of 1000 carbon fibres (T300) of 7 μm diameter. The original cloth thickness is approximately 0.09 mm for the glass cloth and 0.15 mm for the carbon cloth. The epoxy resin as a matrix material was heat-resistant aromatic epoxides (TGDDM in Fig. 1a, Sumiepoxy ELM-434) hardened with aromatic amines (DDS in Fig. 1b). The TGDDM-DDS system is anticipated to be quite radiation-resistant among commercially available epoxy resins. The glass cloth and the carbon cloth were treated with a typical silane coupling agent (Fig. 1c) and an epoxy sizing agent, respectively.

Prepreg sheets were prepared before the lamination and completely hardened under the controlled pressure and temperature. The fabricated laminates had dimensions of 500 mm by 500 mm with a thickness of approximately 2 mm and cut into the desired specimen dimensions along the

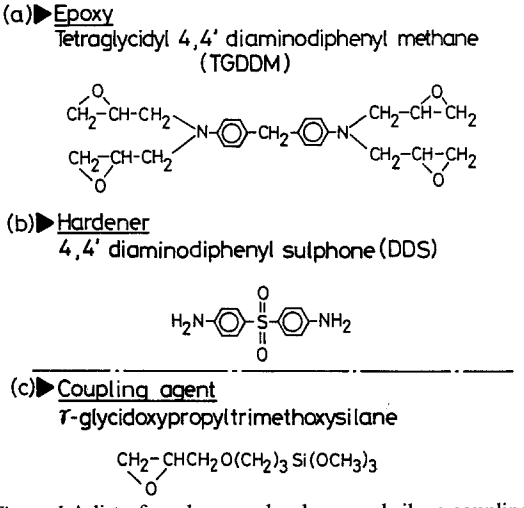

Figure 1 A list of used epoxy, hardener and silane coupling agent.

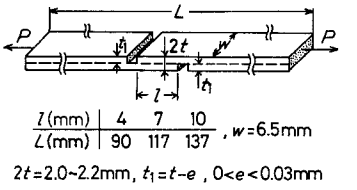

Figure 2 Specimen dimensions for interlaminar tensile shear tests.

two fibre directions. The fibre volume fraction was from 54 to 60%.

2.2. Interlaminar tensile shear tests

Short beam shear strength is most commonly used as a measure of the interlaminar shear strength, but has some disadvantages such as the large effects of loading edges and the complex stress distribution. Here interlaminar tensile shear tests similar to those described in ASTM D-2733 were used to measure the interlaminar shear strength more directly [12, 13]. The specimen dimensions are given in Fig. 2 and the grooves were cut with a diamond-tipped saw. The specimen was gripped at both ends by chucks which were separated by $(l \pm 30)$ mm. Under tension along the specimen length, the shear stress is distributed along the central plane section between the grooves and causes fracture at a critical load. The crosshead speed was 5 mm min^{-1} throughout the study.

2.3. Electron irradiation procedures

Electron irradiation was carried out in air at room temperature with a Dynamitron IEA-300-25-2 type electron accelerator installed at JAERI. Each specimen was wrapped with aluminium foil and attached with a conducting adhesive on the stainless steel plate, which was cooled by cold water during the electron irradiation. The electron acceleration voltage and the beam current were 3 MV and 0.835 mA, respectively. The dose rate was estimated at 0.5 Mrad sec^{-1}. Absorbed dose measurements were made with the CTA (cellulose triacetate) film dosimeter (FTR-125, Fuji Photo Film Co Ltd) [14]. The 125 μm thick CTA films were laminated to measure the dose distribution along the thickness direction. The total absorbed dose given in the following sections is the dose rate (0.5 Mrad sec^{-1}) multiplied by the irradiation time. Composite specimens suffered temperature rise under irradiation and the equilibrium temperature was

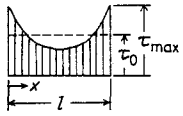

$$\frac{\tau}{\tau_0} = \frac{\theta \cosh(\theta - \frac{2k}{t}x)}{\sinh\theta}$$

$\tau_0 (= \frac{P}{lw})$: mean shear stress

$\theta = \frac{kl}{t}$, $k = (\frac{G'}{2E'})^{1/2}$: mat'l constant

$G'(E')$: "effective" shear(longitudinal) modulus

$$\tau_{max} = \tau_0 \theta \coth\theta \quad \cdots (1)$$

Figure 3 Shear stress distribution along the central plane section between grooves.

measured as $70 \pm 5°$C with an embedded copper-constantan thermo-electric couple.

3. Experimental results and analysis

Markham and Dawson [12] obtained the shear stress distribution along the central plane section between grooves, using a simple shear-lag theory (Fig. 3). The maximum shear stress at the groove edge, τ_{max} ($= \tau|_{x=0,l}$) is given in terms of the average shear stress τ_0 ($= P/lw$) by,

$$\frac{\tau_{max}}{\tau_0} = \theta \coth \theta \qquad (1)$$

$$\theta = \frac{kl}{t},$$

where k is a material constant. It is assumed that the composite laminate fractures when τ_{max} reaches the interlaminar shear strength τ_{crit}, although the actual stress distribution is, of course, far more complex than the simple shear stress state.

A plot of the average shear stress, τ_0, at fracture obtained in the G/E experiments is given in Fig. 4a as a function of the shape parameter l/t. For each total absorbed dose of 0, 3000 and 6000 Mrad, a curve given by Equation 1 was best fitted with the damping Gauss–Newton method and is also shown in Fig. 4a, where the material constant k was fixed ($k = 0.3$) with τ_{max} as an unknown parameter. The values of the maximum shear stress τ_{max} at fracture thus obtained were 6.04, 5.39 and 4.44 kgf mm^{-2} (59.2, 52.9 and 43.5 MPa) for 0, 3000 and 6000 Mrad, respectively. The value of k is not sensitive to the dose and was fixed for simplicity. In order to check the accuracy of the above analysis, the values of τ_{max} were calculated for every sample using Equation 1 with the experimental τ_0 data and the fixed k value, and are shown in Fig. 4b. These calculated values deviate from the dotted line within some reasonable limits.

A plot of τ_0 (mean) and τ_{max} (obtained by the curve fitting) is shown in Fig. 5a for G/E as a function of the total absorbed dose. The interlaminar shear strength decreases as the dose increases. The decrease is particularly pronounced between 2000 and 4000 Mrad. The dose sensitivity almost disappears at more than 6000 Mrad. On the other hand, for C/E, the interlaminar shear strength does not change at least even after 12 000 Mrad as shown in Fig. 5b.

4. Discussion of microscopic fracture mechanisms

Fractured surfaces were observed using a JXA-733 scanning electron microscope. Scanning electron micrographs of laminate centre planes fractured by interlaminar shear are shown for G/E in Fig. 6.

For non-irradiated specimens (Figs. 6a and

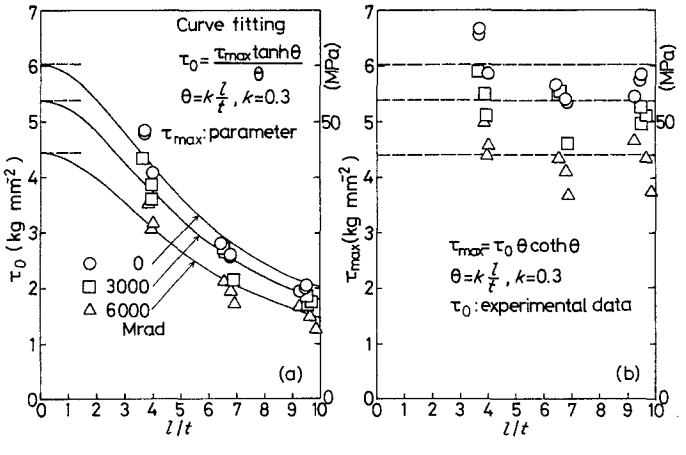

Figure 4 The average shear stress, τ_0, and the maximum shear stress, τ_{max}, at fracture as functions of the shape parameter, l/t, for glass/epoxy laminates irradiated at 70° C. (a) Experimental τ_0 values. The best fitted curve for Equation 1 is also shown, where the material constant k was fixed ($k = 0.3$) with τ_{max} as an unknown parameter. The τ_{max} values can be obtained as the τ_0 values where $l/t = 0$. (b) τ_{max} values calculated for every specimen using Equation 1 with the experimental τ_0 data and the fixed k value ($k = 0.3$).

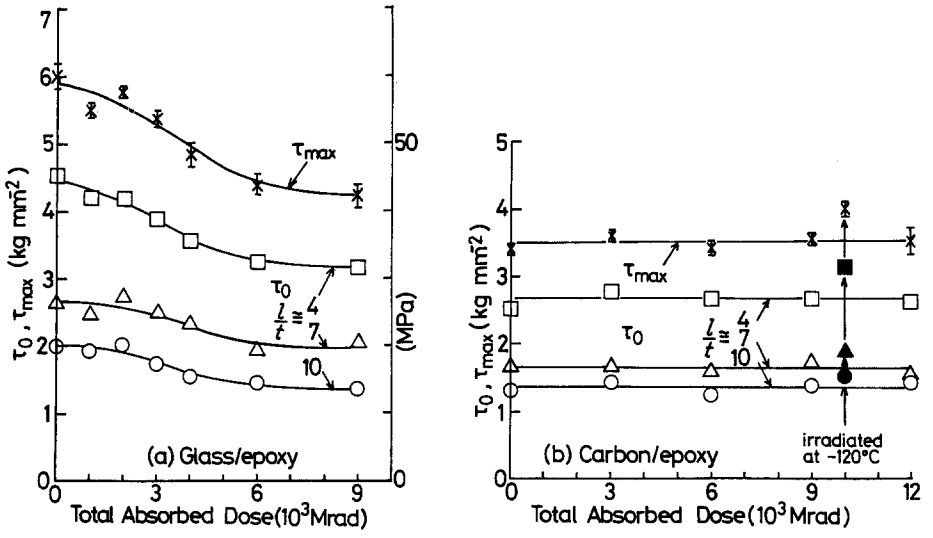

Figure 5 The average shear stress, τ_0, and the maximum shear stress, τ_{max}, at fracture as functions of the total absorbed dose. Irradiation temperature: 70° C. (a) Glass/epoxy. (b) Carbon/epoxy. Data for the −120° C irradiation are also shown.

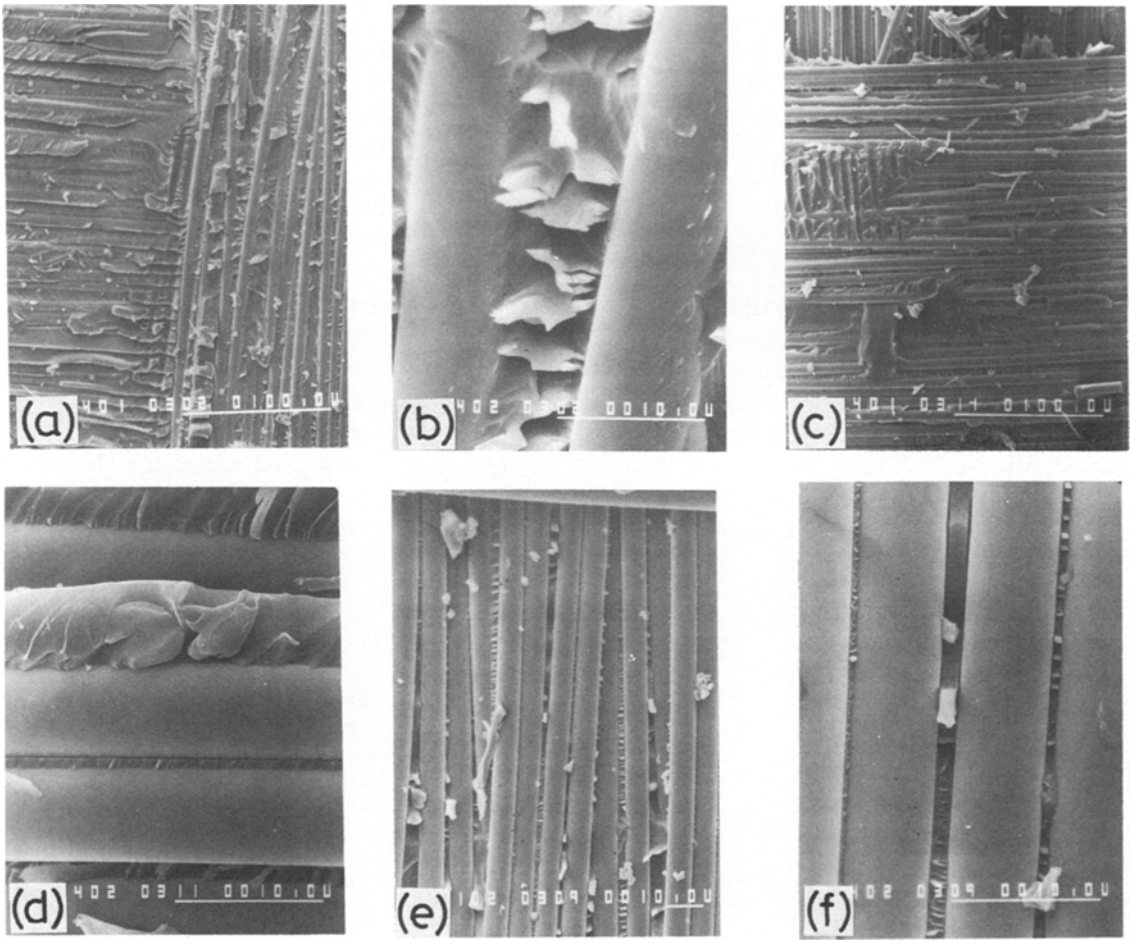

Figure 6 Scanning electron micrographs of central planes of glass/epoxy laminates irradiated at 70° C and fractured by interlaminar shear. (a), (b) Non-irradiated. The adhesion between fibres and resin is good. (c), (d) 3000 Mrad. The interfacial bonding was partially lost. (e), (f) 6000 Mrad. The interfacial bonding was totally lost.

b), the adhesion between fibres and resin is good and the matrix resin is filled between fibres. Some amount of resin still remains on the fibre surfaces. The matrix region consists of rows of "cusps" [15], which are also termed "hackles" (lacerations) [16] that are separated and lifted up from epoxy matrix parallel to one another. The spacings of these evenly distributed cusps or hackles almost correspond to those of fibres. The cusps tend to slant in the same direction as in the fracture or shear loading direction.

On the other hand, after the irradiation of 6000 Mrad (Figs. 6e and f) the adhesion between fibres and resin is lost and gaps can be seen clearly. This debonding or loss of adhesion is considered to be due to loss of silane coupling forces. No resin remains on the fibre surfaces. In addition, resin itself becomes rather brittle and many pieces of debris can also be observed. Both debonding and matrix brittleness are major sources of degradation. Since the adhesion is almost completely lost after the 6000 Mrad irradiation, only friction between matrix and fibres has some resistance to shear forces. The interlaminar shear strengths for the 6000 and 9000 Mrad irradiation are almost the same for this reason.

For specimens after the 3000 Mrad irradiation (Figs. 6c, and d), the fibre–resin adhesion is partly lost, but the remainder is still good. There remain some replicas of debonded fibres on the matrix surface.

The scanning electron micrographs for C/E specimens are shown in Figs. 7a and b for non-irradiated specimens and in Figs. 7c and d after the 12 000 Mrad irradiation. The dose effects do not appear either in the SEM photos or in the interlaminar shear strength data. Presumably this is because the mechanical bonding due to fibre surface roughness forms the major resis-

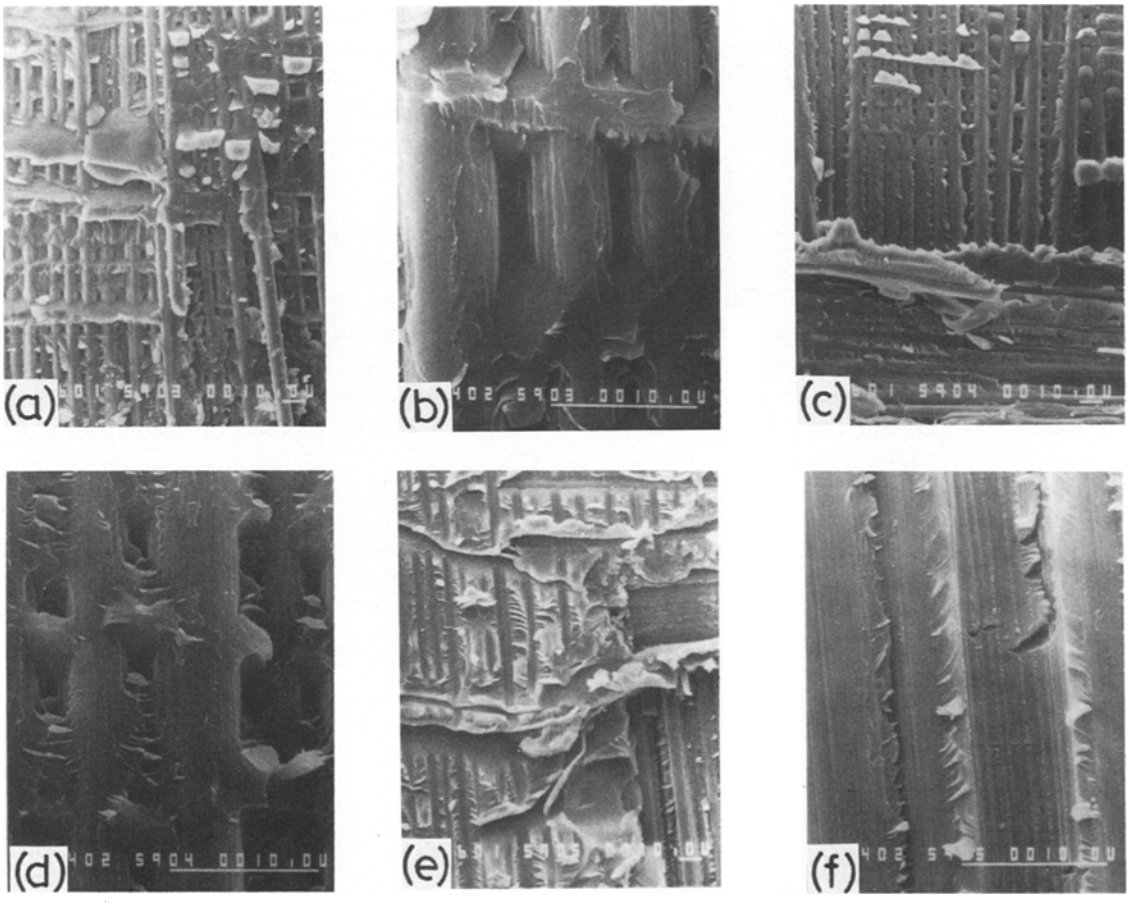

Figure 7 Scanning electron micrographs of central planes of carbon/epoxy laminates fractured by interlaminar shear. (a), (b) Non-irradiated. (c), (d) 12000 Mrad irradiated at 70° C. (e), (f) 1000 Mrad irradiated at −120° C.

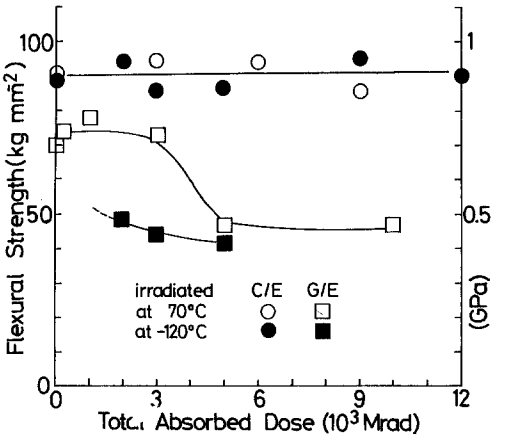

Figure 8 Three-point bending strength as a function of the total absorbed dose. The span-to-thickness ratio is 25.

tance to shear fracture for C/E, not the chemical bonding which presumably is the most important factor for G/E.

5. Comparison with bending test results

The same G/E and C/E laminates as in the interlaminar tensile shear tests were also tested by the three-point bending after the same electron irradiation at 70° C and the results are shown in Fig. 8 by the marks □ and ○. The spans-to-thickness ratio of 25 was used, where the radius of the loading and support noses was 5.08 mm. The crosshead speed was 5 mm min^{-1}. The scanning electron micrograph of G/E and C/E specimens fractured by three-point bending before and after irradiation are shown in Figs. 9a, b and 10a, b, respectively. The bending fracture appearance is different from that of the interlaminar shear fracture, but the interfacial degradation state is similar in both fractures.

For G/E laminates, the bending or flexural strength decreases very rapidly after the dose exceeds 3000 Mrad and approaches a constant value after 6000 Mrad. Judging from the interlaminar shear strength data in Fig. 5a and the bending fracture appearances as shown in Figs. 9a and b, the following deduction can be made for the three-point bending tests of G/E laminates. The bending fracture, which is the fibre fracture of the outermost layer, is dominant up to 3000 Mrad irradiation, but tends to change to the interlaminar shear fracture after around 3000 Mrad.

For C/E laminates, on the other hand, the bending strength is dose-independent. Fracture always occurs by the bending fracture (Figs. 10a and b) since the interlaminar shear strength is also dose-independent.

6. Effects of electron irradiation temperature

Preliminary tests were conducted to observe the effects of electron irradiation temperature which are very important in practice. The schematic view of the liquid nitrogen (LN_2)-cooled low-temperature electron irradiation apparatus is shown in Fig. 11. A Cockcroft–Walton type accelerator (Nishin High Voltage Co, Ltd) installed at JAERI can emit electrons horizontally as well as vertically, and these horizontal electron beams were utilized in the tests. Similarly, as described in Section 2.3, each specimen was wrapped with aluminium foil and attached with a conducting adhesive on the copper plate

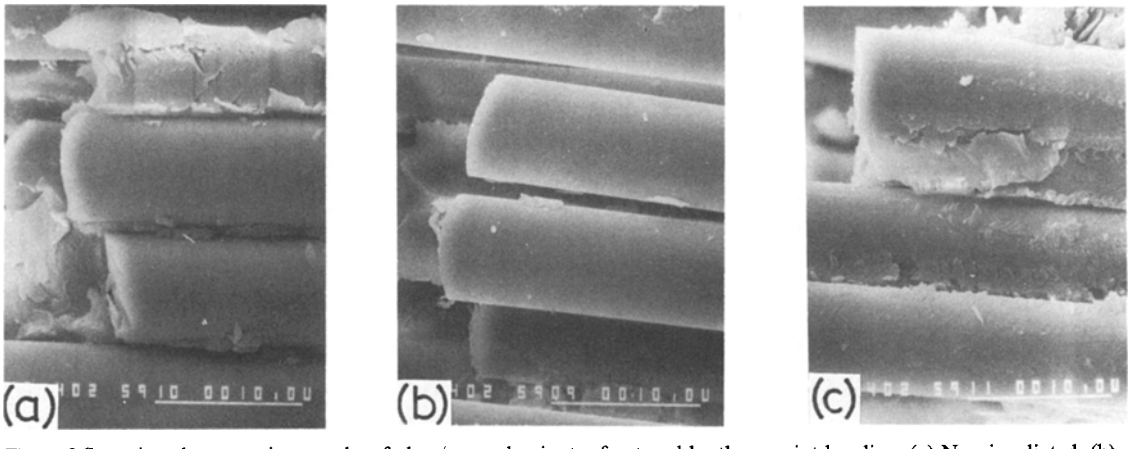

Figure 9 Scanning electron micrographs of glass/epoxy laminates fractured by three-point bending. (a) Non-irradiated. (b) 9000 Mrad irradiated at 70° C. (c) 5000 Mrad irradiated at −120° C.

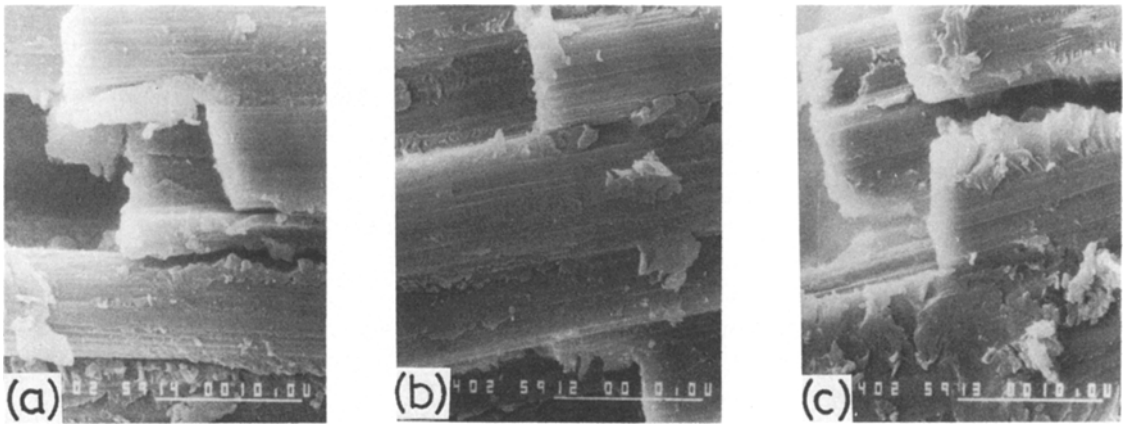

Figure 10 Scanning electron micrographs of carbon/epoxy laminates fractured by three-point bending. (a) Non-irradiated. (b) 9000 Mrad irradiated at 70° C. (c) 13 500 Mrad irradiated at −120° C.

which was cooled by LN_2 in this case. The electron acceleration voltage and the beam current were 1.5 MV and 1 mA, respectively. Similar absorbed dose measurements were conducted again for this experimental setup. The dose rate was estimated at 0.16 Mrad sec^{-1}. The equilibrium temperature during the irradiation was measured as $-120 \pm 10°$ C.

As shown in Fig. 8, the bending strength of G/E laminates irradiated at −120° C was much lower than that irradiated at 70° C. This is presumably due to the decrease in the fibre tensile strength. Fracture appearances show that the fibre fracture of the outermost layer (bending fracture) is always dominant for the −120° C irradation, which is quite different from the 70° C irradiation where the interlaminar shear fracture is dominant over the 3000 Mrad irradiation. Brittle fracture of fibres of G/E bending specimens after the 5000 Mrad irradiation at −120° C can be seen in Fig. 9c, where the fracture surface is perpendicular to the specimen longitudinal axis. For G/E laminates, charge accumulation tends to occur under irradiation since its electrical conductivity may be very low at low temperature. Fracture due to electrical breakdown may have occurred microscopically even without loading. The details of mechanisms of the fibre strength loss are under investigation. Different results may be obtained for the low-temperature gamma irradiation where the charge accumulation is expected to be low because of low dose rate and high power of penetration [17].

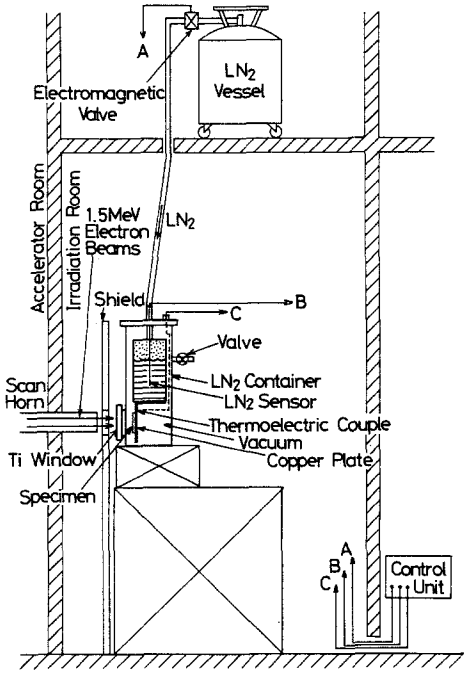

Figure 11 Schematic view of the LN_2-cooled low-temperature electron irradiation apparatus.

For C/E laminates, charge accumulation is not a problem. Three-point bending strength is dose-independent even after the 12 000 Mrad irradiation at −120° C, which is the same for the 70° C irradiation, as shown in Fig. 8. The scanning electron micrograph for the −120° C irradiation (Fig. 10c) shows no difference to those for the 70° C irradiation (Figs. 10a and b). This excellent characteristic of C/E can be very useful in practice. In addition, as shown in Fig. 5b, the interlaminar shear strength of C/E laminates after the 10 000 Mrad irradiation at

$-120°$ C is larger than that for the 70° C irradiation. According to the scanning electron micrographs, fracture occurs mainly in the matrix for the 70° C irradiation (Figs. 7a to d) but in the fibre–matrix interfaces for the $-120°$ C irradiation (Figs. 7e and f). This is a very interesting fact, but the details are still under investigation.

7. Conclusions

Degradation mechanisms of high-energy electron irradiated glass or carbon cloth reinforced epoxy (TGDDM + DDS) laminates were investigated with the interlaminar tensile shear tests and the scanning electron micrographs of fracture surfaces. The following main conclusions were obtained.

1. For glass/epoxy laminates, the interlaminar shear strength decreases significantly after the total absorbed dose exceeds 3000 Mrad. Scanning electron micrographs revealed that debonding of glass fibres and epoxy matrix (or degradation of silane coupling agents) plays an important role in the strength reduction. The decrease in the three-point bending strength after 3000 Mrad corresponds to this decrease in the interlaminar shear strength. Thus, design of the radiation-resistant surface treatment (or silane coupling agents) as well as the resin itself is of supreme importance in order to improve the radiation resistance of glass/epoxy laminates.

2. For carbon/epoxy laminates, both the interlaminar shear and the bending strengths are dose-independent at least up to 12 000 Mrad. Scanning electron micrographs are also almost dose-independent. This excellent characteristic of carbon/epoxy laminates can be very useful in practical applications.

3. Preliminary $-120°$ C irradiation tests were conducted to observe the effects of electron irradiation temperatures, but the details are still under investigation.

Acknowledgements

The authors wish to express their appreciation to the members of the Irradiation Service Section of JAERI-Takasaki for their assistance in the electron irradiation. The authors are also grateful to Sumitomo Bakelite Co Ltd for fabricating composite laminates.

References

1. D. R. TENNEY, *NASA Conf. Proc.* **2251** (1981) 357.
2. R. E. FORNES, J. D. MEMORY and N. NARANONG, *J. Appl. Polym. Sci.* **26** (1981) 2061.
3. B. S. BROWN, *J. Nucl. Mater.* **97** (1981) 1.
4. S. TAKAMURA and T. KATO, *Cryogenics* **20** (1980) 441.
5. R. R. COLTMAN Jr and C. E. KLABUNDE, *J. Nucl. Mater.* **103/104** (1981) 717.
6. S. TAKAMURA and T. KATO, *ibid.* **103/104** (1981) 717.
7. H. W. WEBER, E. KUBASKA, W. STEINER, H. BENZ and K. NYLUND, *ibid.* **115** (1983) 11.
8. C. E. KLABUNDE and R. R. COLTMAN Jr, *ibid.* **117** (1983) 345.
9. S. EGUSA, M. A. KIRK, R. C. BIRTCHER, M. HAGIWARA and S. KAWANISHI, *ibid.* **119** (1983) 146.
10. G. E. HURLEY, J. D. FOWLER and D. L. ROHR, *Cryogenics* **23** (1983) 415.
11. A. UDAGAWA, S. KAWANISHI, S. EGUSA and M. HAGIWARA, *J. Mater. Sci. Lett.* **3** (1984) 68.
12. M. F. MARKHAM and D. DAWSON, *Composites* **6** (1975) 173.
13. C. C. CHIAO, R. L. MOORE and T. T. CHIAO, *ibid.* **8** (1977) 161.
14. R. TANAKA, S. MITOMO, H. SUNAGA, K. MATTSUDA and N. TAMURA, Japan Atomic Energy Research Institute–M report 82-033 (1982).
15. D. PURSLOW, *Composites* **12** (1981) 241.
16. R. RICHARDS-FRANDSEN and Y. NAERHEIM, *J. Compos. Mater.* **17** (1983) 105.
17. S. MATSUOKA, H. SUNAGA, R. TANAKA, M. HAGIWARA and K. ARAKI, *IEEE Trans. Nucl. Sci.* **NS-23** (1976) 1447.

Received 23 July
and accepted 15 October 1984